Low Temperature Physics/Fizika Nizkikh Temperatur, 2022, Vol. 48, No. 3, pp. 254–258

Hybrid shield for microwave single-photon counter based on a flux qubit

V. Yu. Lyakhno, O. G. Turutanov, and A. P. Boichenko

B. Verkin Institute for Low Temperature Physics and Engineering, National Academy of Sciences of Ukraine, Kharkiv 61103, Ukraine
E-mail: turutanov@ilt.kharkov.ua

A. P. Shapovalov, A. A. Kalenyuk, and V. I. Shnyrkov

G. V. Kurdyumov Institute for Metal Physics, National Academy of Sciences of Ukraine, Kyiv 03142, Ukraine

Kyiv Academic University, Kyiv 03142, Ukraine

Received November 8, 2021, revised November 25, 2021, published online January 25, 2022

A scenario of shielding and stabilization of magnetic and electromagnetic fields in the measuring volume occupied by a superconducting flux qubit is considered. The qubit is used as an artificial macroscopic atom with discrete energy levels in a counter of single photons of the microwave range. It is shown that a decrease in the amplitude of variations of the external magnetic field inside the 3-layer hybrid cylindrical shield, composed of superconducting and ferromagnetic cylinders with the diameter-to-length ratio of 1:5, provides high stability of the magnetic field. The absolute value of the magnetic field at the sample location is determined mainly by the magnetic flux captured by the superconductor shields during their superconducting transition. Although the magnetic field stability is more important than the field itself for the photon counter, the paper also discusses experimental methods for reducing the absolute field value in the hybrid shield.

Keywords: magnetic shield, hybrid shield, quantum measurement, flux qubit, single-photon counter.

1. Introduction

The manifestation of quantum coherent phenomena in superconducting devices of macroscopic size makes them attractive from the point of view of creating both scalable circuits for the quantum computer registers and new measuring devices using individual qubits. The typical example is a single-photon counter in the microwave range based on a flux qubit [1]. The regime of quantum dynamics in an “artificial atom” with a discrete Hamiltonian is achieved in macroscopic structures that can be fabricated using modern thin-film technology. However, the macroscopic size of the qubit (gradiometer with loop area of 80×80 μm^2) increases its coupling with the electromagnetic environment that can cause unwanted nonlinear effects such as energy level drift and an increase in the “dark count” rate. This imposes strict requirements on the shielding of the measuring volume in order to reduce the amplitude of variations and provide long-term stabilization of magnetic and electromagnetic fields in the counter location region.

In this work, we discuss the effectiveness of shielding magnetic field and its variation by superconducting and ferromagnetic shields and propose a 3-layer hybrid magnetic shield composed of two superconducting and one ferromagnetic (cryogenic permalloy) coaxial cylinders to provide necessary conditions for the proper functioning of a microwave single-photon detector based on a flux qubit.

2. Attenuation of magnetic field variations by the superconducting cylindrical shield

Let us consider a hollow superconducting cylindrical shield with open ends, length of which is much greater than the diameter, $L \gg 2r$. In the absence of the sources of magnetic fields inside the zero-field-cooled superconducting shield, the problem of the external magnetic field attenuation can be traditionally solved by magnetostatic methods in terms of the scalar magnetic potential V, where magnetic field $\mathbf{B} = -\text{grad}\, V$. Having written the Laplace equation for the scalar magnetic potential V as $\Delta^2 V = 0$ and imposing the boundary condition $\partial V / \partial n = 0$ which describes the diamagnetism of the superconducting cylinder (n is the normal-to-surface coordinate), one can obtain its solution in the form of an infinite Fourier series. In cylindrical coordinates (R, θ, z), its terms contain damping exponents in z, Bessel functions in R, and harmonic functions in θ [2, 3]. Taking into account the symmetry of the problem and being interested in deriving the distribution of the magnetic field along the z axis, we have to keep only the main term in the solution of the Laplace equation and then obtain expressions for the transverse and longitudinal components of the magnetic field. For the transverse component we have

$$B_T(R,\theta,z) = B_T(R,\theta)\exp\left(-1.84\frac{z}{r}\right). \quad (1)$$

Here, 1.84 is the first zero of the derivative of the Bessel function J_1, z is the coordinate having its origin at the open end and directed inside the cylinder, and r is the shield radius. At the point $z = 2r$, the field is attenuated down to $2.528\cdot10^{-2}$ of initial value. The longitudinal (axial) component of the external field decreases much faster with increasing z:

$$B_A(R,\theta,z) = B_A(R,\theta)\exp\left(-3.83\frac{z}{r}\right). \quad (2)$$

This leads to attenuation of the magnetic field with factor $4.84\cdot10^{-4}$ at the same point. Here, the coefficient 3.83 in the exponent is determined by the first zero of the derivative of the Bessel function J_0. From Eqs. (1) and (2), it follows that for a superconducting cylindrical screen with the length $L = (8-10)r$, the variations of the magnetic induction vector can decay by 7–8 orders of magnitude, which ensures high field stability.

Note that formulae (1) and (2) give good estimates for z deep enough inside the shield, since the magnetic field is highly distorted near the open end ($z = 0$) and does not follow from (1) and (2). In practice, long cylinders are used for shielding, so this is not an issue for calculations.

Since the magnetic field is attenuated according to (1) and (2) symmetrically from both open ends of the cylindrical shield, one can make the shield almost half shorter using a cylinder with bottom from one end [4]. The bottom at one end causes a deviation from (1) and (2) only at distances of about r that should be taken into account when mounting a sample.

To observe the dependences (1) and (2) for the absolute field values, one should exclude magnetic flux “trapped” by the shield. The first experimental implementation of such situation was fulfilled at Stanford [5, 6] by mechanically increasing the volume of the shielding shell. With this technique, the absolute values B_x, B_y, B_z of the field components inside the shield can be made as low as $\le 10^{-12}$ T. However, the transition of the shield to the superconducting state almost always occurs in the presence of an external magnetic field, which is partially trapped by the shield. Below we will discuss how to minimize magnetic flux trapping in superconducting shields using an additional permalloy shield.

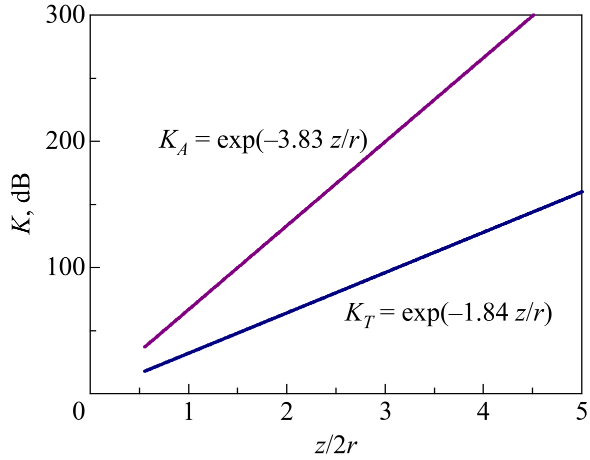

Fig. 1. Theoretical transverse K_T and axial K_A attenuation factors for the magnetic field variations inside the cylindrical superconducting shield along its axis vs. the distance from the cylinder open end, normalized to the diameter calculated by (1) and (2), correspondingly.

Without taking into account the magnetic flux “frozen” in the superconducting shield, expressions (1), (2) well describe the attenuation of external magnetic field variations if make the replacements $\mathbf{B}_T \to \delta\mathbf{B}_T$ and $\mathbf{B}_A \to \delta\mathbf{B}_A$. Figure 1 shows, in a log scale, the transverse and axial attenuation factors for magnetic field variations δB_T, δB_A in the superconducting cylindrical shield as a function of distance z from the open end calculated by formulae (1), (2). Of course, the fields must be less than critical one of the shield material in (1), (2).

The magnitude of the “frozen” field in a superconducting shield depends on many factors: the external field amplitude, the quality of the shield material, and the cooling rate of the shell. So, when the shield is slowly cooled from the closed end, i.e., at an optimal temperature gradient, the magnitude of the field frozen in the shield can be reduced by about two orders of magnitude compared to the external field. Many aspects of the use of superconducting shields can be found in book [4]. We emphasize that if we do not use the technique developed in [5, 6], then the absolute value of the magnetic field inside the shield is not described by expressions (1), (2) because of the magnetic flux trapping effect. The magnetic flux trapped by the shield walls leads to a local field inhomogeneity and an increase in its gradient, which ultimately increases the contribution of vibration-caused noise (“microphone effect”) to the output signal of the counter. Therefore, to reduce the frozen magnetic field, we propose in our work a hybrid design of a cylindrical shield (Fig. 2), composed of two superconducting shells and a cryogenic permalloy shell placed between them.

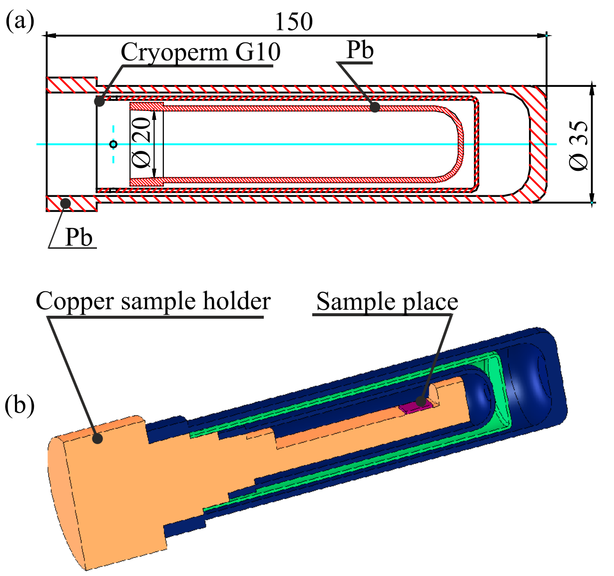

Fig. 2. (a) Hybrid shield schematic with overall sizes and cut view. The wall thickness for the superconducting and permalloy shields are 2 and 1 mm, correspondingly. (b) 3D cut view of the hybrid shield mounted with the sample holder.

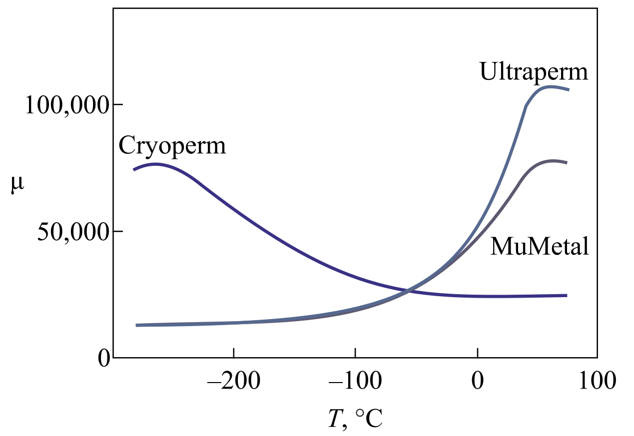

Fig. 3. Magnetic permeability of magnetic shield materials vs. temperature (information from the web site [8]).

3. Magnetic field attenuation by the ferromagnetic cylindrical shield

Being in the fixed residual field of the superconducting shield, the permalloy shield provides a further field reduction inside it. For a cylinder made of permalloy with length L, radius r, wall thickness W and magnetic permeability μ, the attenuation factor of the tangential component of the magnetic field, under the conditions $\mu W(2r)^{-1} \gg 1$ and $W(2r)^{-1} \ll 1$, has the form [7]

$$\gamma_T \approx \mu W(2r)^{-1}. \qquad (3)$$

In our design, these conditions are well met. The attenuation factor for the longitudinal (axial) magnetic field can be represented, using γ_T, in the form

$$\gamma_A \approx 1 + (N/\pi)\gamma_T, \qquad (4)$$

where N is the demagnetization factor for an ellipsoid with the large dimensional ratio $L/2r \gg 1$. It should be emphasized that these formulae are valid only for the case of weak fields that do not lead to saturation effects in permalloy. The saturation induction for permalloy is $B_s \approx 0.5$ T. The outer superconducting shell in the hybrid shield allows this condition to be met. For standard permalloy types 79NM, 81NM, the μ value decreases by an order of magnitude or more with decreasing temperature down to $T = 4.2$ K. This results in a corresponding fall of γ_T. However, in some materials, after a special heat treatment, the magnetic permeability $\mu(T)$ increases significantly with decreasing temperature. An example of such behavior of $\mu(T)$ for cryogenic permalloy Cryoperm® 10 is shown in Fig. 3.

The values of magnetic susceptibility and coercive force at low temperatures for commercial permalloy may differ. Information on specific parameters can be found, for example, in Refs. 8–10. For Cryoperm® 10, the magnetic permeability increases with decreasing temperature and can reach $7.5 \cdot 10^4$. Due to this property, the absolute value of the magnetic induction of the resulting field (the vector sum of the induction of the fields penetrating through the wall and through the open end of the screen) in the Cryoperm® 10 shell at large distances from the open end of the shield decreases by about 60 dB.

Figure 4 shows the plot (in log scale) of the experimentally measured axial component of the magnetic field inside the ferromagnetic cylindrical shield as a function of distance from its open end. The shield was made of Cryoperm® 10

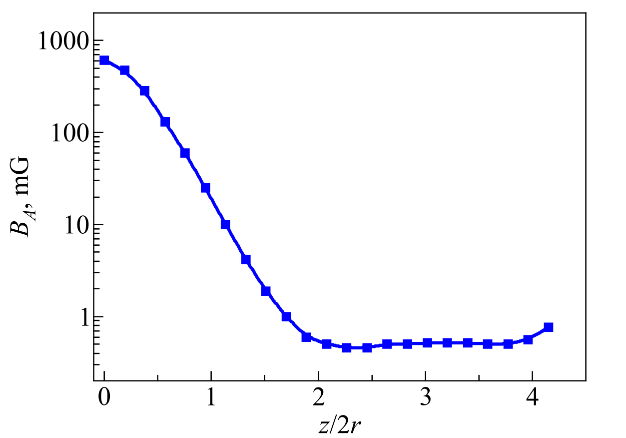

Fig. 4. Attenuation of the Earth's magnetic field component along z axis of the cylindrical Cryoperm® 10 shield. The cylinder has a bottom, its length is 110 mm, the inner diameter is 26.5 mm, and the wall thickness is 1 mm

with the bottom from one end and placed in the natural Earth's magnetic field. The cylinder was oriented horizontally, while the angle between the field vector and the cylinder axis was about 70°. The measurements were carried out on a flux-gate magnetometer MF-20 with a relative error 2.5%. One can see that the attenuated field falls exponentially (with an exponent of 4.06) when moving a sensor inside the shield until it begins rising due to the close end effect. This should be taken into account when designing a multilayer composed shield and choosing the best sample location.

4. Discussion of the hybrid shield

In the design under consideration (Fig. 2), it is important that the internal superconducting screen 100 mm long and 20 mm in diameter, made of lead (Pb), goes into a superconducting state in a weak residual field of the permalloy shield. This significantly reduces the value of the trapped magnetic flux. In addition, since the hybrid shield for the photon counter is located in the dilution refrigerator, the former can be cooled from both the bottom and the top ends. This also leads to a decrease in the trapped magnetic flux, so the resulting attenuated variations in the external magnetic field are well described by the above formulae. The inner lead sheath shields the intrinsic noises of permalloy and further reduces the magnetic field variations at the location of the photon counter by more than 120 dB, as can be calculated from (1) and seen in Fig. 1, if a sample is placed at a distance of $4(z/2r)$, or about 80 mm (see Fig. 2) from the opening of the inner superconducting cylinder. Really, substituting actual value of $z/r=8$ in the exponential function in (1), we have $\exp(-1.84\cdot 8)=\exp(-14.72)\approx 4.05\cdot 10^{-7}$ and, expressing the attenuation factor in decibels, we get $20\lg(4.05\cdot 10^{-7})\approx -128$ dB.

Taking into account the suppression of the uniform magnetic field by the flux qubit design itself by a factor of $\sim 10^4$, the total attenuation coefficient for the magnetic field variations inside the hybrid shield can be estimated as about 200 dB at the counter location. Variations in the magnetic flux in a qubit associated with external noise in the laboratory are negligible, $\delta\Phi < 10^{-9}\Phi_0$ (here $\Phi_0 = h/2e \approx 2.07\cdot 10^{-15}$ Wb is the magnetic flux quantum).

It is well known [6, 10] that the absolute values of the magnetic induction B_T, B_A are minimal at $z\approx(3.5-4)\,(2r)$ and increase when approaching the bottom of the shield. The attenuation coefficient for the absolute magnetic field in this area does not exceed 70 dB. This leads to the fact that the initial magnetic flux in the dc SQUID incorporated in the flux qubit will be $\sim 10^{-4}\Phi_0$, and should be compensated by the control current.

5. Conclusions

The theoretical principles of building quantum computers, including quantum error correction methods, suppressing decoherence, and developing quantum circuits and algorithms, are being successfully elaborated [11]. In practice, however, a number of complicated technological and engineering problems still require their solutions when creating new qubit-based quantum devices or a quantum computer "hardware" [12]. First of all, such tasks include: (i) control over the quality of barriers in Josephson junctions; (ii) suppression of voltage fluctuations on the gates controlling the qubit and reduction of coupling between individual qubit and the magnetic and electromagnetic environment including magnetic shielding and monitoring the residual fields [13]. The considered hybrid shield significantly (200 dB) suppresses the variations of the magnetic field in the qubit location, reduces the absolute value of the field by ~70 dB, and makes it possible to obtain long-term stability of the photon counter characteristics.

This work was carried out within the framework of the project SPS G5796 funded by the NATO and National Academy of Sciences of Ukraine, and the Project No. 0121U110046 funded by the Applied Research Programme of the Ministry of Education and Science of Ukraine.

1. V. I. Shnyrkov, Wu Yangcao, A. A. Soroka, O. G. Turutanov, and V. Yu. Lyakhno, *Fiz. Nizk. Temp.* **44**, 281 (2018) [*Low Temp. Phys.* **44**, 213 (2018)].
2. L. Huang and S. Lee, *Progress in Superconductivity and Cryogenics* **18**(2), 30 (2016).
3. K. Grohmann and D. Hechtfischer, *Cryogenics* **17**, 579 (1977).
4. S. I. Bondarenko and V. I. Sheremet, *Application of Superconductivity in Magnetic Measurements*, Energoatomizdat, Leningrad (USSR) (1982) [in Russian].
5. B. Cabrera and F. J. van Kann, *Acta Astronautica* **5**, 125 (1978).
6. W. O. Hamilton, *Rev. Phys. Appl.* (Paris) **5**, 41 (1970).
7. A. Mager, *J. Appl. Phys.* **39**, 1914 (1968).
8. https://www.mushield.com/material-sales/cryoperm/ (Accessed Nov. 3, 2021).
9. https://vacuumschmelze.com/Company/Quality-and-Safety/Information-for-Manufactured-Articles/CRYOPERM (Accessed Nov. 3, 2021).
10. Yu. Ya. Reutov, *Klassicheskie magnitnye ekrany* [Classic magnetic shields], Ekaterinburg (Russia), UrORAN [Russian Academy of Sciences, Ural division] (2006) [in Russian].
11. I. Tzitrin, J. E. Bourassa, N. C. Menicucci, and K. K. Sabapathy, *Phys. Rev. A* **101**, 032315 (2020).
12. F. Arute, K. Arya, R. Babbush, *et al.*, *Nature* **574**, 505 (2019).
13. A. V. Fedorchenko, V. Yu. Lyakhno, and V. I. Shnyrkov, *SQUID Magnetometer for Structuroscopy of Structural Materials*, *Problems of Atomic Science and Technology* **65**, 150 (2010) [in Russian].

Гібридний екран для лічильника поодиноких НВЧ фотонів на базі потокового кубіту

V. Yu. Lyakhno, O. G. Turutanov, A. P. Boichenko, A. P. Shapovalov, A. A. Kalenyuk, V. I. Shnyrkov

Розглянуто сценарій екранування та стабілізації магнітного та електромагнітного полів у вимірювальному об'ємі, який займає потоковий кубіт. Цей кубіт використовується як штучний макроскопічний атом з дискретними енергетичними рівнями у лічильнику поодиноких фотонів мікрохвильового діапазону. Показано, що зниження амплітуди варіацій зовнішнього магнітного поля всередині тришарового гібридного екрана, який складається з надпровідного та феромагнітного циліндрів з відношенням діаметра до довжини 1:5, забезпечує високу стабільність магнітного поля. Абсолютне значення магнітного поля у місці розташування зразка визначається головним чином магнітним потоком, що був захоплений надпровідними екранами під час їх надпровідного переходу. Хоча стабільність магнітного поля є більш важливою для лічильника фотонів, ніж його значення, у роботі також обговорюються експериментальні методи зменшення абсолютних значень поля у гібридному екрані.

Ключові слова: магнітний екран, гібридний екран, квантове вимірювання, потоковий кубіт, лічильник поодиноких фотонів.